Influence of Different Ligands X^- (X = F, Cl, Br, I, NO_2, CN) on the Rate and Mechanism for Methane Activation by $PtCl_2X_2$ in Aqueous Solution. A Density Functional Theory Study

Hongjuan Zhu and Tom Ziegler*

Department of Chemistry, University of Calgary, 2500 University Drive, N.W., Calgary, Alberta, Canada T2N 1N4

Received November 9, 2006

A density functional study has been carried out on catalytic methane activation by a 1:2 molar mixture of $PtCl_2(H_2O)_2$ and X^- with X = none, F, Cl, Br, I, NO_2, CN. The objective of this study was to better understand the original Shilov experiments, for which a detailed characterization of the active species and the rate determining step has been difficult experimentally. We have found that the rate-determining step for all mixtures is methane uptake rather than C−H activation. Our calculations indicate further that the active species for the weakly coordinating ligands $X^- = Cl^-$, Br^-, I^- are *trans*-$PtCl_2X(H_2O)^-$ and *cis*-$PtX_2Cl(H_2O)^-$, whereas the most abundant complex $PtCl_2X_2^{2-}$ and other species with only halogens have no noticeable activity. For the more strongly coordinating ligands $X^- = F^-$, NO_2^-, CN^-, the most abundant species are $PtCl_2(H_2O)_2$, $PtCl_2X(H_2O)^-$, $PtClX_2(H_2O)^-$, PtX_4^{2-}, and $PtClX_3^-$. Of these species only *cis*-$PtCl_2(H_2O)_2$ and *cis*-$PtCl_2X(H_2O)^-$ are active catalysts for H^+/D^+ exchange. For all the species formed, the free energy barriers of methane and C−H activation have been reported, along with their energy of formation relative to *cis*-$PtCl_2(H_2O)_2$ and X^-.

Introduction

It has been known since the pioneering work by Shilov[1,2] that complexes of late transition metals are able to activate C−H bonds in hydrocarbons. Such an activation is potentially of great interest for industrial functionalization of hydrocarbons (Figure 1a). However, the use of an expensive Pt(IV)-based oxidant has restricted its industrial application. Inexpensive oxidants have been studied by several groups.[3,4] However, limitations of the catalysts, such as low rates and instability, are major obstacles for the industrialization of the Shilov reaction.

The work by Shilov has, on the other hand, prompted several fundamental studies of C−H activation based on experimental methods.[5−7] However, only a few of these studies have focused on the $PtCl_4^{2-}$ and $PtCl_2(H_2O)_2$ species, which were used originally by Shilov in the H^+/D^+ exchange experiment of Figure 1b. This is presumably because the species involved in Figure 1b are difficult to characterize experimentally. Thus, it has not been established experimentally, to the best of our knowledge, whether the rate-determining step in the Shilov H^+/D^+ exchange reactions of Figure 1b is the uptake of CH_4 or the activation of the C−H bond.

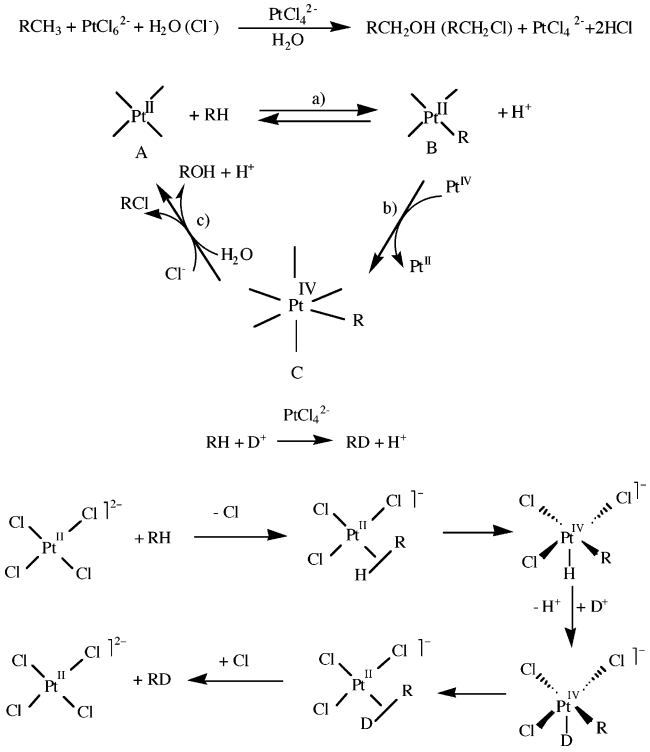

Figure 1. (a, top) Catalytic cycle proposed by Shilov for the platinum-catalyzed oxidation of alkanes in aqueous solution. (b, bottom) Mechanism for H−D exchange reaction discovered by Shilov.

(1) Gol'dshleger, N. F.; Tyabin, M. B.; Shilov, A. E.; Shteinman, A. A. *Zh. Fiz. Khim. (Engl. Transl.)* **1969**, *43*, 1222.

(2) Gol'dshleger, N. F.; Es'kova, V. V.; Shilov, A. E.; Shteinman, A. A. *Zh. Fiz. Khim. (Engl. Transl.)* **1972**, *46*, 785.

(3) (a) Horvath, I. T.; Cook, R. A.; Millar, J. M.; Kiss, G. *Organometallics* **1993**, *12*, 8. (b) Basickes, N.; Hogan, T. E.; Sen, A. *J. Am. Chem. Soc.* **1996**, *118*, 13111.

(4) (a) Freund, M. S.; Labinger, J. A.; Lewis, N. S.; Bercaw, J. E. *J. Mol. Catal. A: Chem.* **1994**, *87*, L11. (b) Rostovtsev, V. V.; Henling, L. M.; Labinger, J. A.; Bercaw, J. E. *Inorg. Chem.* **2002**, *41*, 3608.

(5) (a) *Chem. Rev.* **2001**, *101*, 953 and references therein. (b) Stahl, S.S.; Labinger, J. A.; Bercaw, J. E. *Angew. Chem., Int. Ed.* **1998**, *37*, 2180. (c) Labinger, J. A.; Bercaw, J. E. *Nature* **2002**, *417*, 507.

(6) (a) Procelewska, J.; Zahl, A.; Eldik, R. V.; Zhong, H. A.; Labinger, J. A.; Bercaw, J. E. *Inorg. Chem.* **2002**, *41*, 2808. (b) Jensen, M. P.; Wick, D. D.; Reinartz, S.; White, P. S.; Templeton, J. L.; Goldberg, K. I. *J. Am. Chem. Soc.* **2003**, *125*, 8614.

(7) (a) Johansson, L.; Tilset, M.; Labinger, J. A.; Bercaw, J. E. *J. Am. Chem. Soc.* **2002**, *122*, 10846. (b) Heyduk, A. F.; Driver, T. G.; Labinger, J. A.; Bercaw, J. E. *J. Am. Chem. Soc.* **2004**, *126*, 15034. (c) Heyduk, A. F.; Labinger, J. A.; Bercaw, J. E. *J. Am. Chem. Soc.* **2003**, *125*, 6366.

10.1021/om061035w CCC: $37.00
Publication on Web 03/28/2007

We have, in an attempt to get a more detailed understanding of the original Shilov system, carried out a series of theoretical studies. We were able to show, in the first investigation,[8] that CH_4 uptake rather than C−H activation was the rate-determining step in H^+/D^+ exchange with $PtCl_4^{2-}$ and $PtCl_2(H_2O)_2$ as the catalysts. We were also able to demonstrate that $PtCl_3(H_2O)^-$ is the most active species.

Shteinman et al.[9] studied the influence of different ligands on the H^+/D^+ exchange of the platinum complexes in the Shilov reaction. They used platinum complexes of the type $PtCl_2S_2$ and changed S through a series of ligands with increasing trans-labilizing power ($H_2O < F^- < Cl^- < Br^- < I^- < NO_2^- < PPh_3 < CN^-$). They found that the H^+/D^+ exchange rate decreased in the order $H_2O > F^- > Cl^- > Br^- > I^- > NO_2^- > PPh_3 > CN^-$. This study demonstrated that the H^+/D^+ exchange rate depends inversely on the trans-labilizing power of the ligand S. Thus, Shteinman referred to the inverse trans-labilizing effect in H^+/D^+ exchange as a function of the ligand S in $PtCl_2S_2$.

In this paper, we will study the above inverse trans-labilizing effect of platinum catalysts in the Shilov reaction and examine whether the rate-determining step is still methane uptake, as found in our previous theoretical study on $PtCl_2(H_2O)_2$, or whether the nature of the rate-determining step changes with different ligands S. We hope in addition to identify the most active species for each $PtCl_2S_2$ system after it has been added to water.

Computational Details

Results were obtained from DFT calculations on the basis of the Becke−Perdew exchange-correlation functional,[10−12] using the Amsterdam density functional (ADF) program.[13] The standard double-ζ STO bases with one set of polarization functions were applied for H, N, F, Br, C, and O atoms, while the standard triple-ζ basis sets were employed for the Cl, I, and Pt atoms. The 1s electrons of N, C, F, and O, as well as the 1s−2p electrons of Cl, 1s−3d electrons of Br, 1s−4d electrons of I, and 1s−4f electrons of Pt, were treated as a frozen core. A standard set of auxiliary s, p, d, f, and g STO functions, centered on each nucleus, was used to fit the electron density and calculate the Coulomb and exchange potentials in each SCF cycle. The reported energies include first-order scalar relativistic corrections.[14] Gas-phase electronic enthalpies were calculated from the Kohn−Sham energies. In all free energy values reported, the electronic entropy was neglected and standard expressions[15] were used to calculate the remaining gas-phase enthalpic and entropic contributions at nonzero temperature, including the zero-point vibrational contribution.

Thermodynamic parameters for the solvation of the halogen ions were obtained from a recent compilation of experimental values.[16] The remaining solvation enthalpies were obtained using the COSMO method[17] as implemented in ADF.[18] The solvent excluding surface was used along with an ϵ value of 78.4 for the dielectric constant of water as the solvent. Atomic radii employed were 1.39, 1.8, 1.16, 1.4, 1.3, 2.3, 1.96, 1.33, and 2.2 Å for Pt, Cl, H, N, O, C, Br, F, and I, respectively. Although the Born energy reported by the COSMO model is, strictly speaking, a free energy, the entropic contribution amounts to perhaps 2% of the total energy.[19] The solvation enthalpy was therefore taken as the difference between the gas-phase energy and that calculated using the COSMO solvation model.

For the purpose of calculating the remaining solvation entropies, the solvation process was broken up into three steps, following the method of Wertz.[20] Here, the solute in the gas phase is first compressed to the molar volume of the solvent. The compressed solute gas then loses the same fraction of its entropy as would be lost by the solvent in going from gas (at its liquid-phase density) to liquid. Finally, the solute gas is extended to the concentration of the desired solution (i.e., 1.0 mol/L).

The solute entropy change for the first and third steps, which are strictly changes in molar volume, is given by $\Delta S = R \ln(V_{m,f}/V_{m,I})$, where $V_{m,f}$ is the final solute molar volume and $V_{m,i}$ is the intial solute value. The entropy fraction α lost in the second step can be determined from the absolute entropies of the solvent in its gas ($S_{gas}°$) and liquid ($S_{liq}°$) phases, as shown in eq 1.

$$\alpha = \frac{S_{liq}° - (S_{gas}° + R \ln V_{m,liq}/V_{m,gas})}{S_{gas}° + R \ln V_{m,liq}/V_{m,gas}} \quad (1)$$

Substituting the appropriate parameters for water,[21] we have $\alpha = -0.46$. The sum of the entropy changes accompanying each of the three steps then gives the total solvation entropy; at a temperature of 298.15 K, we have (again, for water) eq 2.

$$\Delta S_{sol} = (-14.3 \text{ cal mol}^{-1} \text{ K}^{-1}) - 0.46(S° - 14.3 \text{ cal mol}^{-1} \text{ K}^{-1}) + (7.98 \text{ cal mol}^{-1} \text{ K}^{-1}) \quad (2)$$

It is convenient that (by chance) the constant terms independent of $S°$ in eq 2 nearly cancel on expansion, and the solvation entropy in water can therefore be approximated in more qualitative discussions as 50% of the gas-phase entropy $S°$, with the opposite sign.

Results and Discussion

In the study[9] by Shteinman of the H^+/D^+ exchange reaction (Figure 1b), 0.0043 mol of $PtCl_2(H_2O)_2$ and 0.0086 mol of X^- (X = F, Cl, Br, I, NO_2, CN) were added to 1 L of D_2O. Thus, the initial concentration of X^- was twice that of $PtCl_2(H_2O)_2$. The anions can replace ligands (H_2O and Cl^-) in $PtCl_2(H_2O)_2$ and form platinum complexes with different groups (S = H_2O, F^-, Cl^-, Br^-, I^-, NO_2^-, CN^-). In the study of the Shilov H^+/D^+ exchange reaction (Figure 1b) presented here, both the alkane uptake and the C−H bond cleavage will be investigated computationally for the different platinum species produced in the Shteinman experiment,[9] where $PtCl_2(H_2O)_2$ is mixed with different anions. Although the dissociative mechanism was found in a previous paper to gives a lower energy barrier,[8] only the associative mechanism will be considered here, because it matches better with the experimental results of the original Shilov reaction. An elaborate discussion of the associative and dissociative mechanisms was given in a previous investigation.[8] Alkanes will be modeled by methane.

(8) Zhu, H.; Ziegler, T. *J. Organomet. Chem.* **2006**, *691*, 4486.
(9) Gol'dshleger, N. F.; Shteinman, A. A. *React. Kinet. Catal. Lett.* **1977**, *6*, 43.
(10) Becke, A. *Phys. Rev. A* **1988**, *38*, 3098.
(11) Perdew, J. P. *Phys. Rev. B* **1986**, *34*, 7406.
(12) Perdew, J. P. *Phys. Rev. B* **1986**, *33*, 8822.
(13) te Velde, G.; Bickelhaupt, F. M.; Baerends, E. J.; van Gisbergen, S.; Guerra, C. F.; Snijders, J. G.; Ziegler, T. *J. Comput. Chem.* **2001**, *22*, 931.
(14) Ziegler, T.; Tschinke, V.; Baerends, E. J.; Snijders, J. G.; Ravenek, W. *J. Phys. Chem.* **1989**, *93*, 3050.
(15) McQuarrie, D. A. *Statistical Thermodynamics*; Harper: New York, 1973.
(16) Fawcett, W. R. *J. Phys. Chem. B* **1999**, *103*, 11181.
(17) Klamt, A.; Schuurmann, G. *J. Chem. Soc., Perkin. Trans. 2* **1993**, 799.
(18) Pye, C. C.; Ziegler, T. *Theor. Chem. Acc.* **1999**, *101*, 396.
(19) Dasent, W. E. *Inorganic Energetics*; Penguin: Middlesex, U.K., 1970.
(20) Wertz, D. H. *J. Am. Chem. Soc.* **1980**, *102*, 5316.
(21) Lide, D. R. *CRC Handbook of Chemistry and Physics*, 76th ed.; CRC Press: New York, 1995.

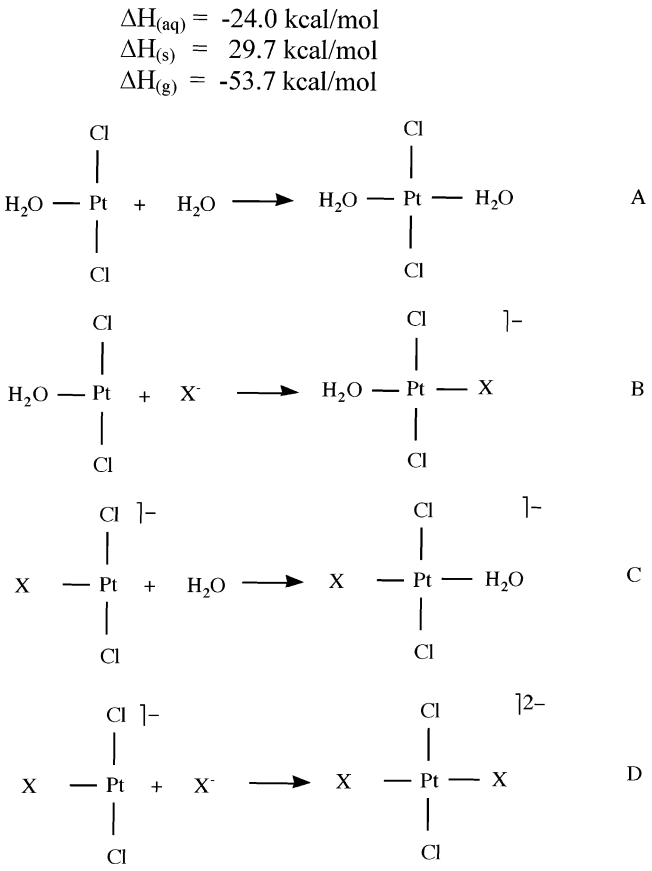

Figure 2. Substitution reactions involving $Pt(H_2O)_nCl_mX_{4-m-n}$ (X = F, Cl, Br, I, NO_2, CN).

Thermodynamics of $Pt(H_2O)_nCl_mX_{4-n-m}$ Species (X = F, Cl, Br, I, NO_2, CN). The addition of $PtCl_2(H_2O)_2$ to water or to an aqueous solution containing the anion X^- (X = F, Cl, Br, I, NO_2, CN) leads to a complex mixture of species in equilibrium with each other. It is only possible to understand this equilibrium by considering the strengths of the different Pt−X bonds and the role played by the ligand trans to X in determining this strength.

We can in general express the bond formation enthalpy for the process

$$(L_nPt)_{aq} + (Y)_{aq} \rightarrow (L_nPt{-}Y)_{aq} \quad (3)$$

as

$$\Delta H_{aq}(Pt{-}Y) = \Delta H_g(Pt{-}Y) + \Delta H_s(Pt{-}Y) \quad (4)$$

where

$$\Delta H_g(Pt{-}Y) = H_g(L_nPt{-}Y) - H_g(L_nPt) - H_g(Y) \quad (5)$$

is the bond formation enthalpy in the gas phase, and

$$\Delta H_s(Pt{-}Y) = H_s(L_nPt{-}Y) - H_s(L_nPt) - H_s(Y) \quad (6)$$

is the change in solvation energy due to the process in eq 3. Formation enthalpies ($\Delta H(Pt{-}Y)$) for stable bonds are negative. It is more common to describe the strength of a bond in terms of the bond dissociation enthalpy (or bond energy) $-\Delta H(Pt{-}Y)$, where a large positive value indicates a strong bond.

When $PtCl_2(H_2O)_2$ is added to an aqueous solution with or without the anion X^-, a number of substitution steps can take place (see steps A−D of Figure 2). The first step (A of Figure 2) involves the dissociation of H_2O from $PtCl_2(H_2O)_2$. We find that the energy required to dissociate one molecule of H_2O from $PtCl_2(H_2O)_2$ is $-\Delta H_{aq}(Pt{-}H_2O) = 24$ kcal/mol in solution. In the gas phase the required energy is as high as $-\Delta H_g(Pt{-}H_2O) = 53.7$ kcal/mol. Thus, solvation effects aid this process by $-\Delta H_s(Pt{-}H_2O) = -29.7$ kcal/mol. The solvation stabilization is a result of *trans*-$PtCl_2(H_2O)$ having a larger solvation energy than *trans*-$PtCl_2(H_2O)_2$ due to the smaller size and more exposed metal center of the former. In the second step (step B of Figure 2), X^- adds to *trans*-$PtCl_2(H_2O)^-$. This process is highly exothermic (Table 1). In the gas phase, the exothermicity ($-\Delta H_g(Pt{-}X)$) follows the order F ≈ CN > NO_2 ≫ Cl > Br > I, which primarily reflects that $2p_\sigma$ orbitals of the first long main-group period have better bonding overlaps with $5d_\sigma$ on the metal center than the np_σ orbitals of the subsequent periods. The exothermicity is reduced in aqueous solution due to the loss of solvation energy by X^-. This reduction (by $-\Delta H_s(Pt{-}X)$) is largest for X = F and follows the order F ≫ Cl > Br > NO_2 ≈ I ≈ CN. This order reflects that the volume that contains the negative charge is smaller for F, Cl, and Br than for NO_2, I, and CN. In the end the Pt−X bond strength in aqueous solution follows the trend CN ≫ NO_2 > F > Cl > Br ≈ I.

Table 1. Bond Formation Enthalpies[a] in $Pt(H_2O)_n(Cl)_mX_{4-n-m}$ (X = F, Cl, Br, I, NO_2, CN)

		X					
reacn		F	Cl	Br	I	NO_2	CN
B[b]	ΔH_{aq}	−38.2	−31.3	−30.0	−29.5	−57.1	−77.1
	ΔH_s	86.9	62.1	58.1	51.9	55.3	51.1
	ΔH_g	−125.1	−93.4	−88.2	−81.4	−112.3	−128.2
C[c]	ΔH_{aq}	−14.6	−10.6	−10.4	−9.5	−5.1	−3.6
	ΔH_s	12.4	11.8	10.6	9.2	14.1	20.2
	ΔH_g	−27.1	−22.3	−21.0	−18.7	−19.3	−23.8
D[d]	ΔH_{aq}	−26.2	−15.3	−14.3	−11.5	−26.8	−34.7
	ΔH_s	−13.4	−35.5	−38.4	−44.4	−30.8	−19.4
	ΔH_g	−12.8	20.2	24.1	32.9	4.0	−15.2

[a] Energy in kcal mol^{-1}. [b] Pt−X in *trans*-$PtCl_2(H_2O)X^-$; see step B of Figure 2. [c] Pt−H_2O in *trans*-$PtCl_2(H_2O)X^-$; see step C of Figure 2. [d] Pt−X in *trans*-$PtCl_2X_2^{2-}$; see step D of Figure 2.

The dissociation of another H_2O molecule from *trans*-$PtCl_2X(H_2O)^-$ (the reverse of step C in Figure 2) leads to the formation of *trans*-$PtCl_2X^-$, which can coordinate another X^- to form *trans*-$PtCl_2X_2^{2-}$ (step D of Figure 2). The calculated H_2O dissociation enthalpy $-\Delta H_{aq}(Pt{-}H_2O)$ for *trans*-$PtCl_2X(H_2O)^-$ follows the order $F^- \gg Cl^- > Br^- > I^- > NO_2^- > CN^-$ for the anions examined here (Table 1). This is what one might expect from the experimentally established order for the trans-labilizing power of the anions $F^- < Cl^- < Br^- < I^- < NO_2^- < CN^-$. However, the trend in the trans-labilizing power differs from gas phase to aqueous solution (Table 1). In the gas phase the Pt−H_2O bond strength with X in the trans position follows the order $I^- \approx NO_2^- < Br^- < Cl^- < CN^- < F^-$ (Table 1). This is also the order of decreasing donor ability we would expect for X^-, at least among the halides. In solution, the Pt−H_2O bond strength depends not only on the differential stabilization of $PtCl_2(H_2O)X^-$ by donation of charge from X^- to the metal center but also on how X influences the solvation energy of $PtCl_2(H_2O)X^-$. Among the halides, solvent effects do not change the order of the Pt−H_2O bond strength or the trans-labilizing power (Table 1). However, it does reduce the difference among F^-, Cl^-, Br^- and I^- compared to the differences in the gas phase. On the other hand, $PtCl_2(H_2O)X^-$ is greatly stabilized by solvation for X = CN and to a lesser extent for X = NO_2 in comparison to the halides (Table 1). The result is that the Pt−H_2O bond strength in solution is smaller for X = CN, NO_2 than for the halides. It should be clear from

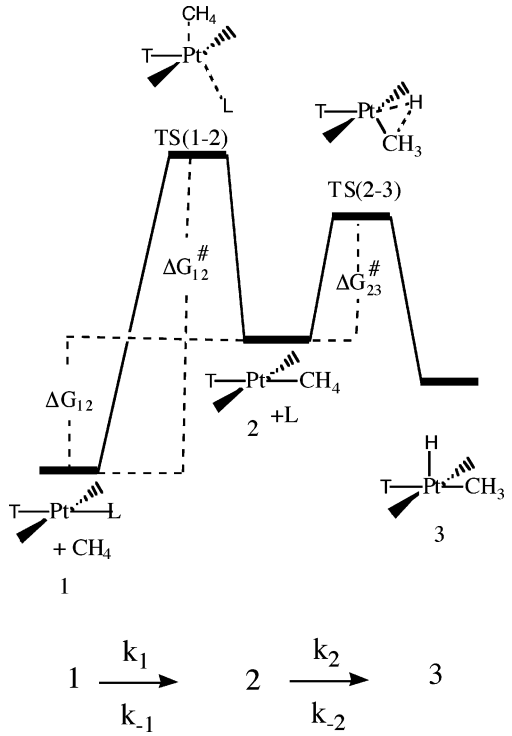

Figure 3. Energy profile for methane activation process.

Scheme 1. Mechanism and Overall Rate of the Associative Uptake of Methane by a Square-Planar Platinum Complex

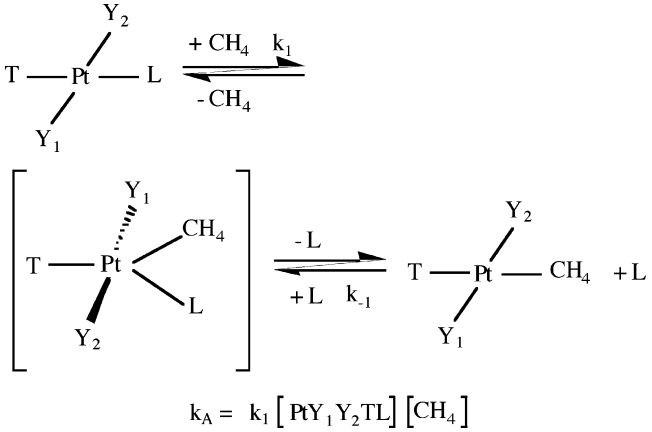

the discussion given here that the so-called trans-labilizing power of a ligand in solution is the product of both electronic factors and solvation effects.

The enthalpy ΔH_{aq}(Pt−X) for the capture of X^- by *trans*-$PtCl_2X^-$ follows in absolute terms the order CN ≫ NO_2 > F > Cl > Br ≈ I, the same as for the capture of X^- by $PtCl_2(H_2O)$ (Table 1). However, the fact that one X ligand in case D of Figure 2 now also is the trans ligand, instead of H_2O as in case B, reduces the Pt−X bond formation energy in absolute terms for case D, especially for the strongly trans-labilizing ligands X = NO_2, CN (Table 1). We shall shortly use the thermodynamic data presented here to discuss the abundance of the different species generated from the addition of $PtCl_2(H_2O)_2$ to a pure aqueous solution or to a solution containing an anion X^- (X = F, Cl, Br, I, NO_2, CN). However, before we do this, we shall discuss the activity of these species toward methane.

The activation of methane takes place in two steps, as shown in Figure 3. In the first step **1** → **2**, methane substitutes associatively (Scheme 1) a ligand L in a square-planar platinum complex. The free energy of reaction of this step is ΔG_{12}, and the corresponding barrier is $\Delta G^{\ddagger}_{12}$. In the second step a C−H bond of the coordinated methane is activated to produce the methyl hydrido complex **3**. The internal barrier for the C−H activation step **2** → **3** is $\Delta G^{\ddagger}_{23}$. However, in order to decide which of the two steps **1** → **2** and **2** → **3** is rate determining, we must compare the uptake barrier $\Delta G^{\ddagger}_{12}$ with the absolute C−H activation barrier $\Delta \bar{G}^{\ddagger}_{23} = \Delta G_{12} + \Delta G^{\ddagger}_{23}$ (Figure 3). We have for a given X studied 10 different activation reactions of methane (**1** → **2** → **3** of Figure 3) (see Schemes 2 and 3). They are numbered 1−10 in Table 2. For each methane activation reaction we have two rows in Table 2. The first gives the uptake barrier $\Delta G^{\ddagger}_{12}$ for the corresponding uptake reactions I[X]−X[X] illustrated in Figure 3. The second row affords the internal ($\Delta G^{\ddagger}_{23}$) and absolute ($\Delta \bar{G}^{\ddagger}_{23}$) C−H activation barrier with $\Delta G^{\ddagger}_{23}$ given in parentheses. The C−H activation paths are numbered 1[X]−5[X] and illustrated in Scheme 4. The methane activation reactions (1−10) each have a different uptake path (I[X]−X[X]), but some have the same C−H activation pathway (1[X]−5[X]). We shall now first discuss the uptake barriers given at the first row of each activation process for different X = F, Cl, Br, I, NO_2, CN in Table 2.

Methane Uptake. Only the associative mechanism is considered here for methane uptake, because this mechanism was found best to fit experimental data for alkane uptake on the basis of the previous calculations.[8] In the associative mechanism (Scheme 1), methane is approaching and the leaving ligand is departing from the platinum center at the same time, leading to the formation of a trigonal-bipyramidal transition state. Subsequently, complete dissociation of the leaving ligand takes place with the formation of a square-planar methane complex.

Free activation energies for methane uptake by $PtCl_n(H_2O)_{4-n}$ species are shown in Scheme 2, whereas the corresponding uptake barriers for the $Pt(H_2O)_nCl_mX_{4-n-m}$ (X = F, Cl, Br, I, NO_2, CN) are given in Table 2. The first four entries in Table 2 involve the $PtCl_2X_2^{2-}$ species formed from the substitution of two H_2O molecules by two X^- ions. The two distinct conformations of $PtCl_2X_2^{2-}$ can give rise to four different uptake paths of CH_4. In I[X], Cl^- is the leaving group and X^- is the trans ligand. For the halogens, the substitution barriers follow the trend expected from the order of their trans-labilizing power. However, X = CN^- is seen to have a higher barrier than X = I^-, although CN^- has the higher trans labilizing power. For II[X] the roles of X^- and Cl^- have interchanged and the barriers are now determined by the Pt−X bond strength. This is also the case for IV[X], where X^- is both the leaving group and the trans group. When Cl^- is both the leaving group and the trans group as in III[X], the dependence of the substitution barrier on X^- is modest. In the next four entries, considerations are given to the species $PtCl_2X(H_2O)^-$ and $PtClX_2(H_2O)^-$, where X^- has substituted one H_2O and one H_2O and one Cl^- ion, respectively. We consider here only cases where H_2O is the leaving group, as it forms a weaker bond to platinum than do the other ligands involved. When Cl^- is the trans ligand (V[X] and VIII[X]), the dependence on X is modest, whereas the trend in the barriers when X is the trans ligand (VI[X] and VII[X]) among the halogens is in line with their trans-labilizing power. The barrier is again higher for CN^- than what would be expected on the basis of its trans-labilizing power. We have finally considered the species in which three or four ligands have been replaced by X^-. In IX[X], X^- is the trans ligand and Cl^- the leaving ligand, whereas X^- is both the trans ligand and leaving ligand in X[X]. We find in both cases the expected dependence on X among the halides, whereas the barrier of substitution for X = CN (IX[X]) is higher than expected. It is quite clear from

Scheme 2. Methane Uptake Pathways and Free Energies of Activation (kcal/mol) for the Abundant Platinum Complexes Generated When $PtCl_2(H_2O)_2$ Is Added to H_2O

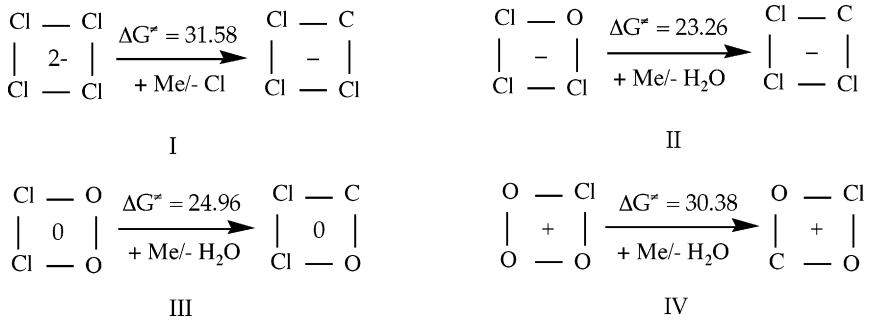

Scheme 3. Methane Uptake Pathways for the Abundant Platinum Complexes Generated When $PtCl_2(H_2O)_2$ Is Mixed in Aqueous Solution with External Ions X^- (X = F, Cl, Br, I, NO_2, CN)

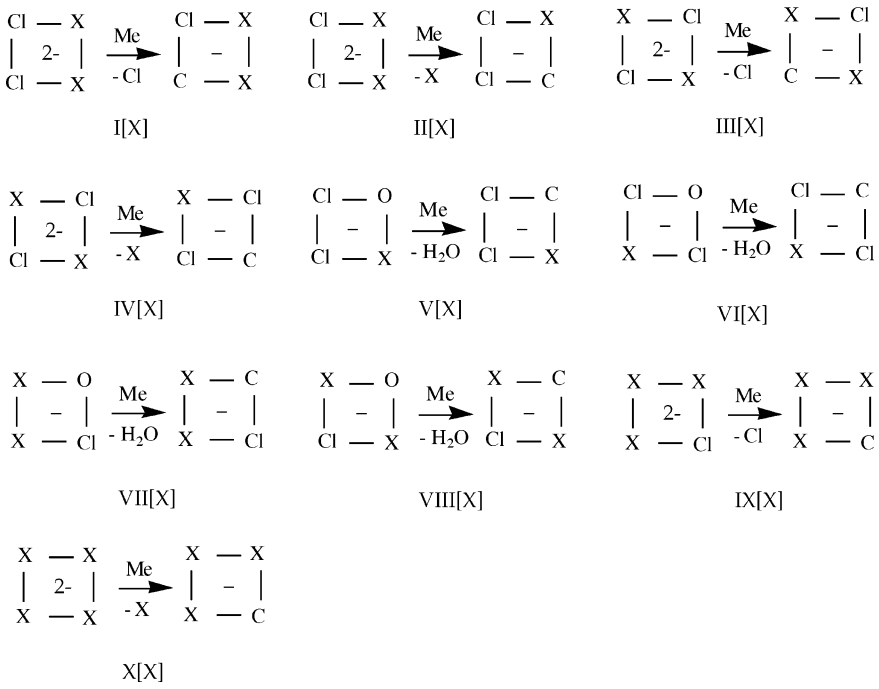

our investigation of methane substitution barriers (Schemes 2 and 3 and Table 2) that the general trends readily can be understood from trends in Pt−X bond energies and the order of the trans-labilizing power of X. The most active species for methane uptake is, according to our analysis, complexes with one or two H_2O ligands situated trans to X.

C−H Activation by $Pt(H_2O)_nCl_mX_{4-n-m}$ (X = F, Cl, Br, I, NO_2, CN). We discuss next the C−H activation step for which we have examined the five different processes 1[X]−5[X] for various ligands X = F, Cl, Br, I, NO_2, CN. Their internal barriers ($\Delta G^{\ddagger}_{23}$ of Figure 3) are given in parentheses in Table 2, and the processes are shown in Scheme 4. For 1[X], 4[X], and 5[X] we have X trans to CH_4. In addition, 4[X] and 5[X] have one or two X ligands cis to CH_4. For X = halogen, the internal barriers for C−H activation are modest (1−3 kcal/mol). The barriers are further seen to increase with the trans-labilizing power of the halogen (F < Cl < Br < I, and the number of X ligands in the cis position has hardly any influence on $\Delta G^{\ddagger}_{23}$ (Table 2).

For the strongly labilizing ligands X = NO_2, CN, we find internal barriers of 16.8−19.8 kcal/mol for NO_2 and 32.4−35.1 kcal/mol for CN. The barriers increase marginally with the number of ligands in the cis position. For the remaining two C−H activation paths, we have Cl^- trans to CH_4 with two (2[X]) and one (3[X]) X ligands in the cis position. The barriers are, as expected, low (1−6 kcal/mol). However, it is interesting to note that they are highest for X = NO_2, CN and largest with two of these ligands in the cis position (Table 2).

We shall finally discuss whether methane uptake (**1** → **2** of Figure 3) or C−H activation (**2** → **3** of Figure 3) is the rate-determining step in the 10 methane activation processes (1−10 of Table 2). For such a discussion, it is required to compare $\Delta G^{\ddagger}_{12}$ for the uptake with $\Delta \bar{G}^{\ddagger}_{23} = \Delta G_{12} + \Delta G^{\ddagger}_{23}$ for C−H activation. The barrier $\Delta \bar{G}^{\ddagger}_{23}$ is shown in the second row after each entry 1[X]−10[X] outside the parentheses. For all those processes (2, 3, 5, 8) where methane is trans to chlorine, we find that methane uptake is rate determining, independent of X. For those reactions (1, 2, 6, 7, 9, 10) where methane is situated trans to X = F, Cl, Br, I, we find that methane uptake is rate determining. However, for X = NO_2, CN, our calculations indicate a shift in the rate-determining step from methane uptake to C−H activation.

It should be pointed out that, while some species with X = NO_2, CN would activate methane with C−H activation rather than methane uptake as the rate-determining step, such species might not be important for the catalytic H^+/D^+ exchange reaction of Figure 1b in an aqueous solution where X = NO_2, CN is added to $PtCl_2(H_2O)_2$. This point will be the subject of

Table 2. Calculated Free Energies of Activation for Associative Methane Uptake and Subsequent C−H Activation by Abundant Platinum Species Formed in a Aqueous Solution of $PtCl_2(H_2O)_2$ with External Ion X^- (X = F, Cl, Br, I, NO_2, CN)

			energy barrier (ΔG)[d−g]					
methane activation reacn[c]	uptake pathway[a]	addition pathway[b]	X = F	X = Cl	X = Br	X = I	X = NO_2	X = CN
1	I[X]		36.8[e]	31.6	30.4	27.5	30.1	32.4
		4[X]	10.3[g] (0[f])	12.9 (1.1)	14.7 (2.0)	13.7 (3.0)	14.1 (16.8)	51.1 (32.8)
2	II[X]		34.1	31.6	29.6	27.6	45.6	68.3
		3[X]	25.2 (0.8)	12.9 (1.1)	16.4 (1.4)	12.3 (0.9)	36.1 (1.9)	62.4 (3.3)
3	III[X]		30.6	31.6	31.8	33.8	28.0	33.8
		2[X]	12.7 (1.3)	12.9 (1.1)	13.7 (1.2)	12.2 (0.8)	19.0 (1.8)	25.2 (6.4)
4	IV[X]		38.7	31.6	31.1	27.2	43.2	55.8
		1[X]	25.6 (0)	12.9 (1.1)	17.3 (2.1)	15.0 (3.6)	49.9 (16.6)	73.9 (28.6)
5	V[X]		25.3	23.3		25.6	25.1	25.3
		3[X]	10.7 (0.8)	10.1 (1.1)		9.9 (0.9)	15.9 (1.9)	14.0 (3.3)
6	VI[X]		31.3	23.3	23.4	22.0	20.9	24.9
		1[X]	9.4 (0)	10.1(1.1)	11.5 (2.1)	12.7 (3.6)	28.4 (16.6)	42.3 (28.6)
7	VII[X]			23.3		21.7	20.2	
		4[X]		10.1 (1.1)		11.7 (3.0)	32.4 (16.8)	
8	VIII[X]			23.3	23.9	23.6		
		2[X]		10.1 (1.1)	10.7 (1.2)	9.5 (0.8)		
9	IX[X]		34.4	31.6	31.4	29.8	29.2	30.9
		5[X]	9.2 (0)	12.9 (1.1)	14.6 (1.8)	12.5 (2.4)	34.4 (19.8)	54.6 (35.1)
10	X[X]		36.7	31.6			42.7	56.3
		5[X]	21.7 (0)	12.9 (1.1)			54.6 (19.8)	89.0 (35.1)

[a] For numbering of uptake reactions I[X]−X[X], see Scheme 3. [b] For numbering of C−H activation reactiond 1[X]−5[X], see Scheme 4. [c] Each methane activation reaction consisted of a uptake path I[X]−X[X] and a C−H activation path 1[X]−5[X]. [d] ΔG in kcal mol^{-1} at 298 K. [e] Free energy of activation for methane uptake, $\Delta G^{\ddagger}_{12}$ of Figure 3. [f] Internal free energy barrier for C−H activation, $\Delta G^{\ddagger}_{23}$ of Figure 3. [g] Absolute free energy barrier for C−H activation, $\Delta \bar{G}^{\ddagger}_{23} = \Delta G_{12} + \Delta G^{\ddagger}_{23}$ of Figure 3.

Scheme 4. C−H Activation by Platinum Methane Complexes Formed after the Methane Uptake of the Abundant Platinum Species When $PtCl_2(H_2O)_2$ Is Added to H_2O (1−3) or an Aqueous Solution Containing an Anion X^- with X = F, Cl, Br, I, NO_2, CN

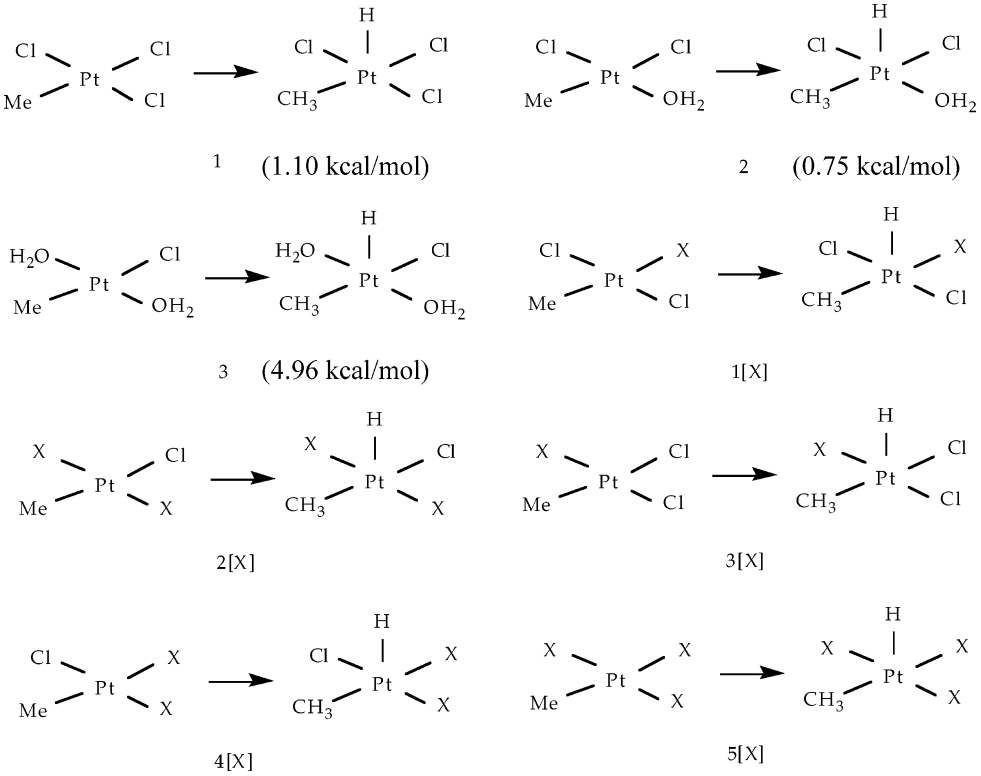

the next section, where we discuss which species actually are responsible for the catalytic H^+/D^+ exchange reaction in an aqueous solution of $PtCl_2(H_2O)_2$ with or without X^- added.

Methane Activation in an Aqueous Solution of $PtCl_2(H_2O)_2$ without an External Anion X^-. When 0.0043 mol is dissolved in 1 L of water (D_2O) without addition of any X^- anions, our calculation shows that disproportion displacement reactions take place with H_2O to form $PtCl_4^{2-}$ (0.1%), $PtCl_3(H_2O)^-$ (10.9%), $PtCl_2(H_2O)_2$ (78.2%), $PtCl(H_2O)_3^+$ (10.6%), and $PtCl_4^{2-}$ (0.2%). The overall rate of H^+/D^+ exchange K in this mixture can be expressed as

$$K = \sum_i k_i \qquad (7)$$

Table 3. Relative Free Energy, Distribution, and Rate Contribution to H^+/D^+ Species Generated from the Mixing[a] of $PtCl_2(H_2O)_2$ in Water with X^- (X = F, Cl, Br, I, CN, NO_2)

		X					
species		F	Cl	Br	I	NO_2	CN
$PtCl_2(H_2O)_2$	ΔG[b]	0/−0.23	0/−0.23	0/−0.23	0/−0.23	0/−0.23	0/−0.23
	c_i[c]	12.2 (5.2/7.0)	0.0 (0/0)	0.1 (0/0.1)	0.0 (0/0)	11.0 (4.7/6.3)	12.4 (5.2/7.2)
	$\bar{k}_{a,i}$[d]	0.2 (0.2/0)				0.13 (0.13/0)	0.15 (0.15/0)
$PtCl_2X(H_2O)^-$	ΔG	−19.7/−19.8	−4.91	−4.8/−9.2	−6.2/−7.1	−34.5/−34.2	−48.2/−54.7
	c_i	25.7 (10.9/14.8)	13.9	9.4 (0/9.4)	20.0 (4.6/15.4)	24.3 (10.3/14.0)	25.8 (10.9/14.9)
	$\bar{k}_{a,i}$	0.2 (0.2/0)	3.9	2.2 (0/2.2)	22.3 (0.1/22.2)	0.24 (0.24/0)	0.19 (0.19/0)
$PtCl_2X_2^{2-}$	ΔG	−35.0/−35.9	−7.72	−15.0/−15.0	−8.6/−9.4	−56.5/−55.7	−96.6/−86.3
	c_i	26.4 (11.0/15.4)	86.0	78.0 (42.0/36.0)	62.3 (16.3/46.0)	16.7 (1.4/15.3)	26.9 (11.3/15.6)
	$\bar{k}_{a,i}$	∼0.0	∼0.0	∼0.0	∼0.0	∼0.0	∼0.0
$PtClX_3^{2-}$	ΔG	−48.53		−16.92	−7.70	−74.06	−128.04
	c_i	18.4		7.2	4.3	15.1	18.8
	$\bar{k}_{a,i}$	∼0.0		∼0.0	∼0.0	∼0.0	∼0.0
PtX_4^{2-}	ΔG	−61.59		−18.87	−7.11	−94.24	−162.51
	c_i	15.9		1.1	1.3	15.6	15.9
	$\bar{k}_{a,i}$	∼0.0				∼0.0	∼0.0
$PtClX_2(H_2O)^-$	ΔG	−32.5/−33.0		−7.0/−12.0	−6.7/−6.6	−55.1/−52.4	−93.0/−77.1
	c_i	1.4 (0.8/0.6)		4.5 (0/4.5)	12.0 (6.3/5.7)	17.3 (16.9/0.4)	0.18 (0.18/0)
	$\bar{k}_{a,i}$			0.6	14.9 (13.9/1.0)	∼0.0	
X^-	c_i	6.6×10^{-7}	14.0	0.15	13.1	1.0×10^{-9}	9.2×10^{-18}
Cl^-	c_i	51.6	-	13.9	19.0	63.49	50.7
K[e]		0.4	3.9	2.8	37.2	0.37	0.34

[a] In the mixing, one portion of $PtCl_2(H_2O)_2$ was added to two portions of X^- in l L of D_2O. [b] Free energy in kcal mol^{-1} relative to $PtCl_2(H_2O)_2$ and X^-. [c] Percent of initial $PtCl_2(H_2O)_2$ concentration $A_0 = 4.3 \times 10^{-3}$ mol L^{-1}. [d] Contribution from species i to overall rate (see eq 8b). [e] Total rate of all species (see eq 9).

Here k_i is the rate (not rate constant) of H^+/D^+ exchange for species i. It follows from the discussion in the previous sections that the rate-determining step in the H^+/D^+ exchange reaction for platinum species that only contain water and halides is the methane uptake. We can thus in eq 7 replace k_i with $k_{a,i}$, representing the rate (not rate constant) of associative methane uptake k_a (see Scheme 1) for species i. Thus

$$K = \sum_i k_{a,i} = \sum_i k_{1,i} \times A_0(c_i/100)[CH_4] \qquad (8a)$$

Here $k_{1,i}$ is the rate constant for associative uptake of methane (Scheme 1). Further, c_i is the calculated percent abundance of species i and $A_0 = 4.3 \times 10^{-3}$ mol L^{-1} is the initial concentration of $PtCl_2(H_2O)_2$. It should be mentioned that the rate expression for associative methane uptake

$$k_{a,i} = k_{1,i}A_0(c_i/100)[CH_4] \qquad (8b)$$

used in eq 8a is derived under the assumption that C−H activation is much faster than the reverse reaction of methane uptake so that $k_2 > k_{-1}$ in Figure 3. The actual rate $\bar{K}$ given by Shteinman[9] at 100 °C is normalized with respect to the initial concentration of A_0 in $PtCl_2(H_2O)_2$ as

$$\bar{K} = K/A_0 = \sum_i k_{a,i}/A_0 = \sum_i \bar{k}_{a,i} = \sum_i k_{1,i}(c_i/100)[CH_4] \qquad (9)$$

We find for $PtCl_2(H_2O_2)$ in aqueous solution $\bar{K} = 4.0 \times 10^{-3}$ L mol^{-1} s^{-1}, in good agreement with the value obtained by Shteinman[9] of 6.3×10^{-3} L mol^{-1} s^{-1}. Only two species contribute to $\bar{K}$, namely $PtCl_2(H_2O)_2$ with $k_{i,1}[CH_4] = 2.81 \times 10^{-3}$ L mol^{-1} s^{-1} and $PtCl_3(H_2O)^-$ with $k_{i,2}[CH_4] = 27.87 \times 10^{-3}$ L mol^{-1} s^{-1}. The overall contribution to the rate of H^+/D^+ exchange is $\bar{k}_{a,1} = 0.93 \times 10^{-3}$ L mol^{-1} s^{-1} for the more abundant and less active $PtCl_2(H_2O)_2$ and $\bar{k}_{a,2} = 3.03 \times 10^{-3}$ L mol^{-1} s^{-1} for the more active and less abundant $PtCl_3(H_2O)^-$.

Methane Activation in an Aqueous Solution of $PtCl_2(H_2O)_2$ with an External Anion X^-. We shall now turn to the case where we add $PtCl_2(H_2O)_2$ to aqueous solution of X^- with X = F, Cl, Br, I, NO_2, CN. Table 3 affords in the first column the species formed when $PtCl_2(H_2O)_2$ and X^- are mixed. The next columns provide for each X the free energy of the species and its isomers relative to *cis*-$PtCl_2(H_2O)_2$ and X^-, the percent abundance, and the total contribution $\bar{k}_{a,i}$, and the individual contribution of each isomer from the species i to the overall rate $\bar{K}$ for the H^+/D^+ exchange. With the weakly coordinating ligands $X^- = Cl^-$, Br^-, I^-, according to our calculations, we note that the prevalent species formed when one part of $PtCl_2(H_2O)_2$ is mixed with two parts of X^- are $PtCl_2X_2^{2-}$, with 86% (Cl), 78% (Br), 62% (I) abundance. Some water substitution is seen to take place through

$$2PtCl_2X_2^{2-} + H_2O \rightarrow PtClX_3^{2-} + PtCl_2X(H_2O)^- + Cl^- \qquad (10)$$

$$PtCl_2X_2^{2-} + H_2O \rightarrow PtClX_2(H_2O)^- + Cl^- \qquad (11)$$

The species formed in these reactions are $PtClX_3^{2-}$, $PtCl_2X(H_2O)^-$, and $PtClX_2(H_2O)^-$, with energies comparable to that of $PtCl_2X_2^{2-}$ (see Table 3). The two species responsible for catalyzing the H^+/D^+ exchange are the aquo species $PtCl_2X(H_2O)^-$ and $PtClX_2(H_2O)^-$, with a combined calculated abundance of 13.9%, 13.7%, and 32%, respectively, for X = Cl, Br, I. For X = Cl, Br, our calculated rates at $K = 3.9$ and 2.8 L mol^{-1} s^{-1}, respectively, which compare well with the experimental estimates of $\bar{K} = 4.1$ L mol^{-1} s^{-1} for X = Cl and $\bar{K} = 2.47$ L mol^{-1} s^{-1} for X = Br (Table 3). In the case of X = I, we find a rate of $\bar{K} = 37.2$ L mol^{-1} s^{-1}, which is 2 orders of magnitude larger than the experimental estimate of $\bar{K} = 0.40$ L mol^{-1} s^{-1}. Such a deviation is acceptable, as it corresponds to an error in the calculated free energy of activation of 2−3 kcal mol^{-1}. Indeed, it follows from Table 2 that the uptake barriers for $PtCl_2X(H_2O)^-$ and $PtClX_2(H_2O)^-$ is calculated to be ∼2 kcal mol^{-1} lower for X = I than for X = Cl, Br. It is important to point out that all species active in H^+/D^+ exchange for X = Cl, Br, I has methane uptake as the rate-determining step.

For X = NO_2, F, CN, the Pt−X bond is much stronger than the Pt−Cl link. As a result, PtX_4^{2-} and $PtClX_3^{2-}$ are more stable

than $PtCl_2X_2^{2-}$ (Table 3). For this reason substitution reactions such as

$$2PtCl_2X_2^{2-} + H_2O \rightarrow PtClX_3^{2-} + PtCl_2X(H_2O)^- + Cl^- \quad (12)$$

$$2PtCl_2X_2^{2-} + 2H_2O \rightarrow PtClX_4^{2-} + PtCl_2(H_2O)_2 + 2Cl^- \quad (13)$$

become exergonic. However, stoichiometric constraints limit the amount of PtX_4^{2-} and $PtClX_3^{2-}$ that can be formed. The mixture of X^- and $PtCl_2(H_2O)_2$ contains as a consequence a number of species in significant abundance, such as $PtCl_2(H_2O)_2$, $PtCl_2X_2^{2-}$, $PtCl_2X(H_2O)^-$, $PtClX_2(H_2O)^-$, PtX_4^{2-}, and $PtClX_3^{2-}$. Of these species, only *cis*-$PtCl_2(H_2O)_2$ and *cis*-$PtCl_2X(H_2O)^-$ are active as catalysts for H^+/D^+ exchange (Table 3). However, although the combined calculated abundances of the two aquo species are 37.9% (F), 35.3% (NO_2), and 38.3% (CN), respectively, the activities of the two species are low (Table 3). The calculated total exchange rates for X = NO_2, CN are $\bar{K} = 0.37$ and 0.34 L mol^{-1} s^{-1}, respectively, in reasonable agreement with the experimental estimates[7] of $\bar{K} = 0.115$ L mol^{-1} s^{-1} for X = NO_2 and $\bar{K} = 0.106$ L mol^{-1} s^{-1} for X = CN. On the other hand, our theoretical value of $\bar{K} = 0.4$ L mol^{-1} s^{-1} for X = F is somewhat lower than the experimental rate of $\bar{K} = 6.29$ L mol^{-1} s^{-1}. We note again that the deviation is acceptable, since it corresponds to an error in $\Delta G^{\ddagger}_{12}$ of 1−2 kcal mol^{-1}. It is further important to point out that the only active species in the mixture of X^- and $PtCl_2(H_2O)_2$ are *cis*-$PtCl_2(H_2O)_2$, *cis*-$PtCl_2(NO_2)(H_2O)^-$, *cis*-$PtCl_2(F)(H_2O)^-$, and *cis*-$PtCl_2(CN)H_2O^-$. All of these species catalyze the H^+/D^+ exchange in a way where methane uptake is the rate-determining step (Table 2). There are species in the mixture, such as $Pt(NO_2)_4^{2-}$, and $Pt(CN)_4^{2-}$, that potentially would have C−H activation as the rate-determining step. However their activity is too low to make any noticeable contribution to the overall exchange rate.

Concluding Remarks

Shilov[1] demonstrated in 1969 that it is possible for species present in an aqueous solution of $PtCl_4^{2-}$ or $PtCl_2(H_2O)_2$ to activate C−H bonds of alkanes. The scope of Shilov's discovery has been extended by Shteinman and Gol'dshleger[7] to an aqueous solution containing one part of $PtCl_2(H_2O)_2$ and two parts of X^- with X = F, Cl, Br, I, NO_2, CN. In their extended study, Shteinman and Gol'dshleger[7] were able to show that the activity toward H^+/D^+ exchange or alkane activation followed the trend X = none ≈ F > Cl > Br > I > NO_2 ≈ CN in a 1:2 molar mixture of $PtCl_2(H_2O)_2$ and X^-.

The discovery by Shilov has instigated numerous studies on C−H activation by homogeneous catalysts. However, few of these investigations have involved the original systems considered by Shilov and Shteinman, allegedly because these systems are difficult to characterize experimentally in terms of active species. We have in the current study attempted to characterize the Shilov and Shteinman systems by computational means.

The first part of the investigation evaluated the relative free energy of species that can possibly be formed in a 1:2 molar mixture of $PtCl_2(H_2O)_2$ and X^- (Tables 1 and 3). We find for the more weakly coordinating halides X = Cl, Br, I that the prevalent species in the mixture is $PtCl_2X_2^{2-}$, with some presence of $PtCl_2X(H_2O)^-$ and $PtClX_2(H_2O)^-$. For the more strongly coordinating ligands X = F, NO_2, CN we have in addition a substantial abundance of PtX_4^{2-} and $PtClX_3^-$ as well as $PtCl_2(H_2O)_2$.

The second part was concerned with whether methane uptake or C−H activation is the rate-determining step in H^+/D^+ exchange catalyzed by the different species formed in the 1:2 molar mixture of $PtCl_2(H_2O)_2$ and X^- (Scheme 3). In those cases where methane uptake is rate determining for species i, we have according to eq 9 for the rate of methane activation

$$\bar{k}_{a,i} = k_{1,i}(c_i/100)[CH_4] \quad (14)$$

whereas the rate of methane activation due to species i is given by

$$\bar{k}_{CH,i} = k_{2,i}\left(\frac{k_{1,i}}{(k_{-1,i})}\right)(c_i/100)\frac{[CH_4]}{[L]} \quad (15)$$

when C−H activation is the rate-determining step in methane activation. Here L is the ligand displaced by methane in step 1 → 2 of Scheme 3.

By comparing the free energy of activation for methane uptake, $\Delta G^{\ddagger}_{12}$ of Scheme 3, with the absolute free energy barrier of C−H activation, $\Delta \bar{G}^{\ddagger}_{23} = \Delta G_{12} + \Delta G^{\ddagger}_{23}$, we find that all species formed from the weakly coordinating ligands $X^- = Cl^-$, Br^-, I^- catalyze the H^+/D^+ exchange with methane uptake as the rate-determining step (Table 2). The only two species that contributr to the methane activation for X = Cl, Br, I are *trans*-$PtCl_2X(H_2O)^-$ and *cis*-$PtX_2Cl(H_2O)^-$ with water as the leaving group. The much more abundant $PtCl_2X_2^{2-}$ species do not contribute to the methane activation, since the halogens are poorer leaving groups than water and the barrier for methane uptake is as a result higher.

In the group X = F, NO_2, CN of more strongly coordinating X^- ligands, the active species are $PtCl_2(H_2O)_2$ and *cis*-$PtCl_2X(H_2O)^-$ with water as the leaving group. Both species have methane uptake as the rate-determining step in methane activation. No other species have any significant contribution to the H^+/D^+ exchange rate. There are complexes for X = NO_2,CN such as PtX_4^{2-} and *trans*-$PtX_2Cl_2^{2-}$ with X^- as the leaving group as well as PtX_3Cl^{2-} with Cl^- as the leaving group that potentially could have C−H activation as the rate-determining step (Table 2). However, their activity is too low to be of importance. Also the species mentioned above with X^- as the leaving group L might still not have C−H activation as the rate-determining step due to the 1/[L] dependence of $\bar{k}_{CH,i}$ (eq 15) and the low concentration of NO_2^- and CN^- (Table 3).

For CH_4 uptake by T−Pt(Y_1,Y_2)−L high rates are obtained by good leaving groups such as water and strong trans-labilizing ligands. The influence of the Y_1, Y_2 cis ligands is modest. For C−H activation in the complex T−Pt(Y_1,Y_2)−CH_4, the internal barrier goes up with the trans-labilizing power of the trans ligand. We shall in a forthcoming account provide a full discussion on the relation between the trans-labilizing ability of T and the C−H activation barrier based on our energy decomposition scheme.[22]

Acknowledgment. This work was supported by the NSERC. T.Z. thanks the Canadian government for a Canada Research Chair.

OM061035W

(22) Mitoraj, M.; Zhu, H.; Michalak, A.; Ziegler, T. *J. Org. Chem.* **2006**, *71*, 9208.